Inorganic Chemistry

Article

pubs.acs.org/IC

NMR Investigations of Dinuclear, Single-Anion Bridged Copper(II) Metallacycles: Structure and Antiferromagnetic Behavior in Solution

Daniel L. Reger,* Andrea E. Pascui, and Perry J. Pellechia

Department of Chemistry and Biochemistry, University of South Carolina, Columbia, South Carolina 29208, United States

Andrew Ozarowski

National High Magnetic Field Laboratory, Florida State University, Tallahassee, Florida 32310, United States

Supporting Information

ABSTRACT: The nuclear magnetic resonance (NMR) spectra of single-anion bridged, dinuclear copper(II) metallacycles $[Cu_2(\mu\text{-}X)(\mu\text{-}\mathbf{L})_2](A)_3$ ($\mathbf{L}_m$ = *m*-bis[bis(1-pyrazolyl)-methyl]benzene: X = F^-, A = BF_4^-; X = Cl^-, OH^-, A = ClO_4^-; $\mathbf{L}_m$* = *m*-bis[bis(3,5-dimethyl-1-pyrazolyl)methyl]benzene: X = CN^-, F^-, Cl^-, OH^-, Br^-, A = ClO_4^-) have relatively sharp ^1H and ^{13}C NMR resonances with small hyperfine shifts due to the strong antiferromagnetic superexchange interactions between the two $S = {}^1/_2$ metal centers. The complete assignments of these spectra, except X = CN^-, have been made through a series of NMR experiments: $^1H-{}^1H$ COSY, $^1H-{}^{13}C$ HSQC, $^1H-{}^{13}C$ HMBC, T_1 measurements and variable-temperature ^1H NMR. The T_1 measurements accurately determine the Cu···H distances in these molecules. In solution, the temperature dependence of the chemical shifts correlate with the population of the paramagnetic triplet ($S = 1$) and diamagnetic singlet ($S = 0$) states. This correlation allows the determination of antiferromagnetic exchange coupling constants, $-J$ ($\hat{\mathbf{H}} = -J\hat{\mathbf{S}}_1\hat{\mathbf{S}}_2$), in solution for the $\mathbf{L}_m$ compounds 338(F^-), 460(Cl^-), 542(OH^-), for the $\mathbf{L}_m$* compounds 128(CN^-), 329(F^-), 717(Cl^-), 823(OH^-), and 944(Br^-) cm^{-1}, respectively. These values are of similar magnitudes to those previously measured in the solid state ($-J_{solid}$ = 365, 536, 555, 160, 340, 720, 808, and 945 cm^{-1}, respectively). This method of using NMR to determine $-J$ values in solution is an accurate and convenient method for complexes with strong antiferromagnetic superexchange interactions. In addition, the similarity between the solution and solid-state $-J$ values of these complexes confirms the information gained from the T_1 measurements: the structures are similar in the two states.

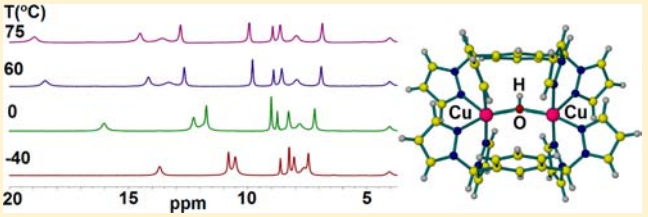

INTRODUCTION

The study of dinuclear copper(II) complexes formed from ligands containing nitrogen donor atoms[1] as models for type-3 active sites of copper enzymes[2] (e.g., tyrosinase, oxyhemocyanin, laccases, ascorbate oxidase, ceruloplasmin) is extensive. In these systems, histidine residues are coordinated to the copper(II) centers with at least one small bridging group directly connecting the metal centers and mediating strong antiferromagnetic superexchange interactions.[3] In addition to the solid-state structural and magnetic information, the characterization of these models in solution is important because of possible applications as biomimetic catalysts[4] and/or molecular magnets.[5]

Paramagnetic copper(II) complexes usually have long electronic relaxation times and give broad nuclear magnetic resonance (NMR) signals, thus impeding characterization in solution.[6] In contrast, dinuclear, antiferromagnetically coupled copper(II) complexes give relatively narrow NMR signals; however, there are only a limited number of examples in the literature that demonstrate the use of this method as a means of characterization in solution.[7,8] In these studies, the small bridging ligand responsible for the antiferromagnetic coupling of the copper(II) centers is usually an OH^- group. Currently, there are no solution studies of an extensive series of dinuclear copper(II) compounds where the structure is held relatively constant while the small bridging anions are varied. Very few examples of these types of copper(II) complexes have been characterized by two-dimensional (2D) NMR techniques ($^1H-{}^1H$ COSY)[8] and apparently there are no examples of ^{13}C NMR and $^1H-{}^{13}C$ correlation studies.

We have recently synthesized a series of five coordinate dinuclear copper(II) metallacycles supported by the ligands *m*-bis[bis(1-pyrazolyl)methyl]benzene ($\mathbf{L}_m$) and *m*-bis[bis(3,5-dimethyl-1-pyrazolyl)methyl]benzene ($\mathbf{L}_m$*) of the formula $[Cu_2(\mu\text{-}X)(\mu\text{-}\mathbf{L})_2](A)_3$ ($\mathbf{L}_m$: X = F^-, A = BF_4^-; X = Cl^-, OH^-, A = ClO_4^-; $\mathbf{L}_m$*: X = CN^-, F^-, Cl^-, OH^-, Br^-, A = ClO_4^-).[9] Scheme 1 shows the structure of the two ligands, which differ by the methyl substitution of the pyrazolyl rings, and Figure 1 shows the structure of the $[Cu_2(\mu\text{-}F)(\mu\text{-}\mathbf{L}_m{}^*)_2]^{3+}$ cation.

The $\mathbf{L}_m$* complexes have unusual structural features, such as the linear Cu−X−Cu bridging arrangement and axially

Received: August 5, 2013
Published: October 11, 2013

   dx.doi.org/10.1021/ic402016m | *Inorg. Chem.* 2013, 52, 12741−12748

Scheme 1. Schematic Representation of the Ligands L_m and L_m*

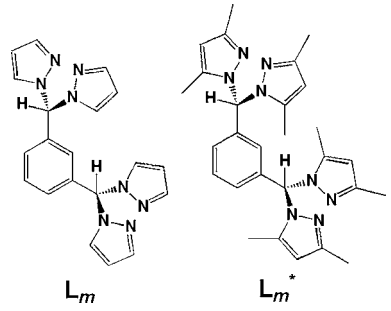

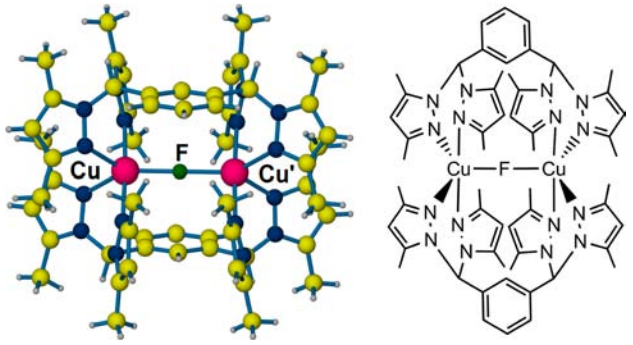

Figure 1. Solid-state structure and drawing of $[Cu_2(\mu\text{-}F)(\mu\text{-}L_m^*)_2]^{3+}$.

compressed trigonal bipyramidal geometry around the metal centers. This arrangement,[9] where the bridging X^- ligand occupies an equatorial site of the coordination sphere, results in strong antiferromagnetic superexchange interactions in the solid state, $-J$ = 160(CN^-), 340(F^-), 720(Cl^-), 808(OH^-), and 945(Br^-) cm^{-1}, respectively ($\hat{H} = -J\hat{S}_1\hat{S}_2$, where $-J$ is the exchange coupling constant) as a result of the overlap of the "donut"-shaped portion of the spin-rich copper(II) d_{z^2} orbitals with the bridging anion orbitals. The magnitude of $-J$ correlates with the size of the bridging halides and it is unusually large for the OH^-.[9a] "Broken-Symmetry" density functional theory (DFT) ORCA calculations showed that as the size of the bridging halide increases, the energy of the triplet state increases faster than the energy of the singlet state, resulting in larger singlet−triplet energy gaps. The hydroxide singlet−triplet gap resides between that of the Cl^- and Br^- bridged compounds. The exchange integral and the spin delocalization of unpaired spin density toward the bridging group also increase as the size of the bridging halide is increasing.

The F^- bridged complex of the L_m ligand has the same trigonal bipyramidal geometry as the analogous L_m* compound, with an almost linear Cu−F−Cu bridging angle (164−180°, depending on the solvent content of the crystals),[9b] and, subsequently, the $-J$ value is similar, 365 cm^{-1} vs. 340 cm^{-1}. The Cu−X−Cu bridging angle in the Cl^-[10] and OH^- analogues is smaller (153.2° and 141.0°) than in the L_m* analogues (180°), resulting in weaker superexchange interactions in the L_m series ($-J$ = 536 and 555 cm^{-1}, respectively) when compared to analogous L_m* compounds (720 and 808 cm^{-1}, respectively) in solid state.

Here we report the determination of the structures in solution, using one-dimensional (1D) and 2D NMR techniques, as well as T_1 measurements for the calculation of Cu···H distances, of this first extensive series of dinuclear copper(II) metallacycles, where the X^- bridges promote strong antiferromagnetic interactions, and where these bridges are systematically varied. We also determine, from variable-temperature (VT) ^{1}H NMR studies, the magnitude of the exchange coupling constant ($-J$) in solution and compare these results with the solid-state $-J$ values previously determined from SQUID measurements.[9b,c]

EXPERIMENTAL SECTION

The ^{1}H, ^{13}C NMR, and 2D NMR (^{1}H−^{1}H COSY, ^{1}H−^{13}C HSQC, ^{1}H−^{13}C HMBC) spectra were recorded on a Varian Mercury/VX 400 or a Bruker Avance-III HD 400 with broadband Prodigy Cryoprobe. All chemical shifts are given in ppm and were referenced to residual undeuterated solvent signals (^{1}H) and deuterated solvent signals (^{13}C). The 2D NMR experiments were run with gradient coherence selection pulse sequences that were included with the vendor supplied software (VNMRJ version 2.2C or Topspin 3.1). The VT experiments were carried out in the temperature range of −40 °C to 75 °C (233−348 K) in acetonitrile-d_3. A standard Varian L900 variable-temperature controller was utilized in these experiments. The longitudinal relaxation times (T_1) were determined by standard inversion−recovery experiments. For the calculated Cu···H distances, from the crystal structures, equivalent hydrogen atoms were averaged. If the two copper(II) centers were not equivalent in solid state, the Cu···H distances were measured from each copper(II) and then were averaged.

MestReNova and SigmaPlot software was used in the preparation of figures.[11]

Syntheses, single-crystal structures of the copper(II) metallacycles, and $-J$ values in solid state, calculated from fitting the magnetic susceptibilities to the Bleaney−Bowers equation, were previously reported or prepared and measured by analogous procedures.[9] *[**Caution**: Although no problems were encountered during this work with the perchlorate salts, these compounds should be considered potentially explosive!]*

RESULTS AND DISCUSSION

NMR Assignments and Confirmation of Structure in Solution. Solid-state magnetic susceptibility measurements demonstrated that the dinuclear copper(II) complexes, $[Cu_2(\mu\text{-}X)(\mu\text{-}L_m)_2](A)_3$ (X = F^-, A = BF_4^-; X = Cl^-, OH^-, A = ClO_4^-) and $[Cu_2(\mu\text{-}X)(\mu\text{-}L_m^*)_2](ClO_4)_3$ (X = F^-, Cl^-, Br^-, OH^-, CN^-), show strong antiferromagnetic coupling,[9] while the ^{1}H NMR spectra of analogous dinuclear Zn(II) and Cd(II) compounds, e.g. $[Cd_2(\mu\text{-}F)(\mu\text{-}L_m^*)_2](ClO_4)_3$, showed that the single anion bridged, metallacyclic structure is retained in solution.[9] For these reasons, we anticipated relatively sharp ^{1}H NMR resonances for these copper(II) compounds, with small hyperfine shifts. The ^{1}H NMR resonances, in CD_3CN at 20 °C, are indeed relatively sharp and in a very narrow chemical shift range for copper(II) complexes: $[Cu_2(\mu\text{-}F)(\mu\text{-}L_m)_2](ClO_4)_3$ 2 to 30 ppm, $[Cu_2(\mu\text{-}Cl)(\mu\text{-}L_m)_2](ClO_4)_3$ 4 to 25 ppm, $[Cu_2(\mu\text{-}OH)(\mu\text{-}L_m)_2](ClO_4)_3$ 4 to 17 ppm, $[Cu_2(\mu\text{-}CN)(\mu\text{-}L_m^*)_2](ClO_4)_3$ −5 to 20 ppm, $[Cu_2(\mu\text{-}F)(\mu\text{-}L_m^*)_2](ClO_4)_3$ −2 to 27 ppm, $[Cu_2(\mu\text{-}Cl)(\mu\text{-}L_m^*)_2](ClO_4)_3$ 0 to 13 ppm, $[Cu_2(\mu\text{-}OH)(\mu\text{-}L_m^*)_2](ClO_4)_3$ 0 to 10 ppm and $[Cu_2(\mu\text{-}Br)(\mu\text{-}L_m^*)_2](ClO_4)_3$ 1 to 8 ppm.

A series of NMR experiments were carried out in order to assign these resonances. First, we recorded the VT ^{1}H NMR spectra in the temperature range −40 °C to 75 °C in acetonitrile-d_3. The shape and position of the resonances are dependent on the population distribution between the diamagnetic singlet S = 0 (ground) and the triplet S = 1 (excited) states; that is, they are essentially a function of the

dx.doi.org/10.1021/ic402016m | Inorg. Chem. 2013, 52, 12741−12748

Table 1. Chemical Shifts and Assignments of the ^{1}H NMR and ^{13}C NMR Resonances of $[Cu_2(\mu\text{-}X)(\mu\text{-}L_m)_2](A)_3$ (X = F^-, A = BF_4^-; X = Cl^-, OH^-, A = ClO_4^-) and $[Cu_2(\mu\text{-}X)(\mu\text{-}L_m{*})_2](ClO_4)_3$ (X = CN^-, F^-, Cl^-, OH^-, Br^-) at 20 °C[a]

	$[Cu_2(\mu\text{-}X)(\mu\text{-}L_m)_2]^{3+}$						$[Cu_2(\mu\text{-}X)(\mu\text{-}L_m{*})_2]^{3+}$									
X	**F^-**		**Cl^-**		**OH^-**		**CN^-**		**F^-**		**Cl^-**		**OH^-**		**Br^-**	
	^{1}H	^{13}C	^{1}H	^{13}C	^{1}H	^{13}C	^{1}H	^{13}C	^{1}H	^{13}C	^{1}H	^{13}C	^{1}H	^{13}C	^{1}H	^{13}C
a or **a*** [a]	9.35[b]		10.96	-	7.88	184.6[b]	-2.82	-	-0.82	-	0.75[e]	11.0	0.19	9.8	1.49	15.7
a or **a*** [a]	24.14[b,c]		17.86	-	12.44	201.9[b]	-4.17	10.1	-1.15[e]	7.3		19.5	1.66	20.5	1.15	10.6
c or **c*** [a]	18.62	184.9 198.2	14.18		9.31	-	-0.30	19.4	1.13	34.2	1.93	18.3	1.95	16.2	2.18	12.6
c or **c*** [a]	15.35		15.92	-	12.10	136.4	1.68	23.8	3.31	21.1	2.70	14.8	2.84	13.1	2.69	11.7
b	24.58		19.83		12.99	162.4	3.42	48.6	9.83	136.1	9.66	125.6[d]	7.63	124.1	7.56	-
b	29.70		24.55		16.98	168.7	4.44	105.8	26.85	-	12.10	-	9.77	-	8.00[c]	-
d	4.82	59.8	5.39	62.5	7.08	70.3	9.42	128.5	10.95	-	6.31	64.3	7.13	66.0	7.13	66.5
f	10.52	128.0	8.43[c]	127.5	8.38	129.6	10.77	129.6	16.79[e]	132.3	8.19[e]	130.3	8.52[e]	131.1	7.68	128.5
g	9.80	134.6	8.56	131.5	8.81	133.2	13.00	134.3				131.9		133.1	7.91	130.1
e	2.67[b]	123.0	4.17	122.9[d]	4.03	123.2[d]	17.66	141.5	4.03	-	4.00	-	3.95	-	4.69	125.4
***ipso*-C**		137.7		135.6[d]		138.2				140.2		136.7		138.0		135.1

[a]See Figure 2 for the labeling scheme of individual hydrogen and carbon atoms. Multiple resonances that were not clearly assigned are shown in one cell. [b]*a**, *c** for the compounds with the ligand L_m* and *a*, *c* for the L_m compounds. [c]Broad resonance. [d]Shoulder. [e]Tentative assignment (no correlation was found in the ^{1}H−^{13}C HSQC spectra). [f]Two resonances merged.

strength of the antiferromagnetic interaction. To facilitate the interpretation of the ^{1}H NMR data, we also recorded the ^{13}C NMR, ^{1}H−^{1}H COSY, ^{1}H−^{13}C HSQC spectra of the compounds and for $[Cu_2(\mu\text{-}OH)(\mu\text{-}L_m{*})_2](ClO_4)_3$ the ^{1}H−^{13}C HMBC spectrum.

To complete and/or confirm the assignments of the ^{1}H NMR resonances, the T_1 spin−lattice relaxation times were measured. Assuming a predominantly paramagnetic dipolar relaxation mechanism[7] for the metallacyclic protons, the distance between the closest paramagnetic copper(II) center and the hydrogen atoms can be determined according to the following equation: $d_i = d_{ref}(T_{1i}/T_{1ref})^{1/6}$, where d_i and T_{1i} are the Cu···H crystallographic distances and spin−lattice relaxation time of proton *i*, similarly d_{ref} and T_{1ref} are the Cu···H distance and spin−lattice relaxation time of a reference hydrogen. The results of this analysis have a 20% error margin.

As the strength of the antiferromagnetic interaction decreases, the assignment of the resonances becomes harder; the 2D NMR experiments, as a result of short nuclear relaxation times, provide less or no useful information. In these cases, the integrals of the deconvoluted resonances and similarities between the spectra of the more weakly and strongly coupled copper(II) complexes were taken into consideration along with the spectra of the d^{10} analogues. The shape and the temperature-dependent behavior of the resonances also facilitate the assignments. The assignments are shown in Table 1, while Figure 2 shows the ^{1}H NMR spectrum of $[Cu_2(\mu\text{-}Br)(\mu\text{-}L_m{*})_2](ClO_4)_3$ at −40 °C, along with a labeled drawing. The labeling scheme shown on the left side of Figure 2 is correct for all L_m* compounds; the L_m compounds are labeled analogously except there are no *a** and *c** methyl groups attached to the pyrazolyl rings.

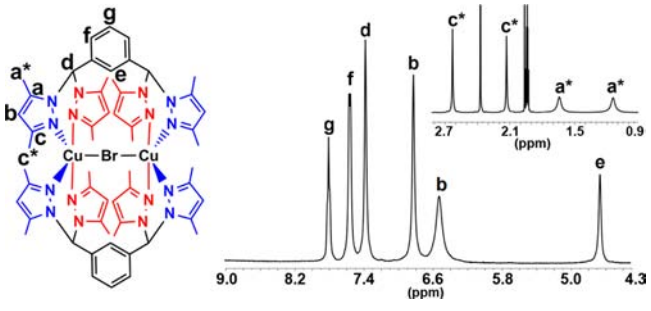

Figure 2. ^{1}H NMR spectrum of $[Cu_2(\mu\text{-}Br)(\mu\text{-}L_m{*})_2](ClO_4)_3$ at −40 °C. Red axial, blue equatorial pyrazolyl rings.

The ^{1}H and ^{13}C NMR spectra of $[Cu_2(\mu\text{-}Br)(\mu\text{-}L_m{*})_2](ClO_4)_3$ at −40 °C show a single resonance for the methines (*d*) and the resonances corresponding to the nonequivalent positions of the phenylene spacers (*e*, *f*, *g*, and *ipso*-C). For the *a**, *c**, and *b*-pyrazolyl resonances, two distinct environments are observed (^{13}C resonances for ring carbon atoms are not observed for the compounds with L_m*) corresponding to the axial and equatorial pyrazolyl rings of the trigonal bipyramidal geometry around copper(II) observed in the solid state.

The VT ^{1}H NMR spectra of $[Cu_2(\mu\text{-}Br)(\mu\text{-}L_m{*})_2](ClO_4)_3$ (see Figure 3) shows the temperature-dependent behavior of the resonances. Most resonances move to lower shielding as the temperature is increased, except the *d* and *a** resonances. The *b*-pyrazolyl resonances are the most affected by the temperature change, especially the broader *b*-resonance, which shifts to lower shielding by more than 3 ppm. The temperature dependent hyperfine shifts correlate with $-J$, this issue is discussed in detail later.

The line widths of *a** and one of the *b*-pyrazolyl resonances are much larger than the *c** and the other *b*-pyrazolyl resonances, presumably because of an increase in paramagnetic relaxation effects causing shorter spin−spin relaxation times. The *a** resonances are closer (ca. 3.7 Å) to the metal centers than the *c** resonances (ca. 5.9 Å), and although the *b*-pyrazolyl resonances in both the axial and equatorial positions are ∼5.0−5.2 Å away from the copper(II) centers, the broad *b*-pyrazolyl resonances can be tentatively assigned to the axial pyrazolyl rings, which are oriented toward the "dumbbell"-shaped region of the spin-rich d_z^2 orbitals of copper(II).

The assignments above are corroborated by the Cu···H distances determined from T_1 measurements at room temperature (Table 2). The *f* resonance was chosen as reference for the calculation of Cu···H distances, because in the ^{1}H−^{1}H COSY spectrum of the $[Cu_2(\mu\text{-}X)(\mu\text{-}L_m{*})_2](ClO_4)_3$ X = CN^-, F^-, Cl^-, Br^-, OH^- compounds, the only peaks, other than the diagonal peaks, expected and observed are the *f* and *g* peaks, δ(7.68,7.91) and δ(7.91,7.68), making the assignments definitive. As shown in Table 2, the distances determined by NMR match those measured by X-ray crystallography quite well. This match in values demonstrates that the structure of $[Cu_2(\mu\text{-}Br)(\mu\text{-}L_m{*})_2](ClO_4)_3$ in solution is similar to the solid-state structure.[9b] Analogous tables for the other compounds can

dx.doi.org/10.1021/ic402016m | Inorg. Chem. 2013, 52, 12741−12748

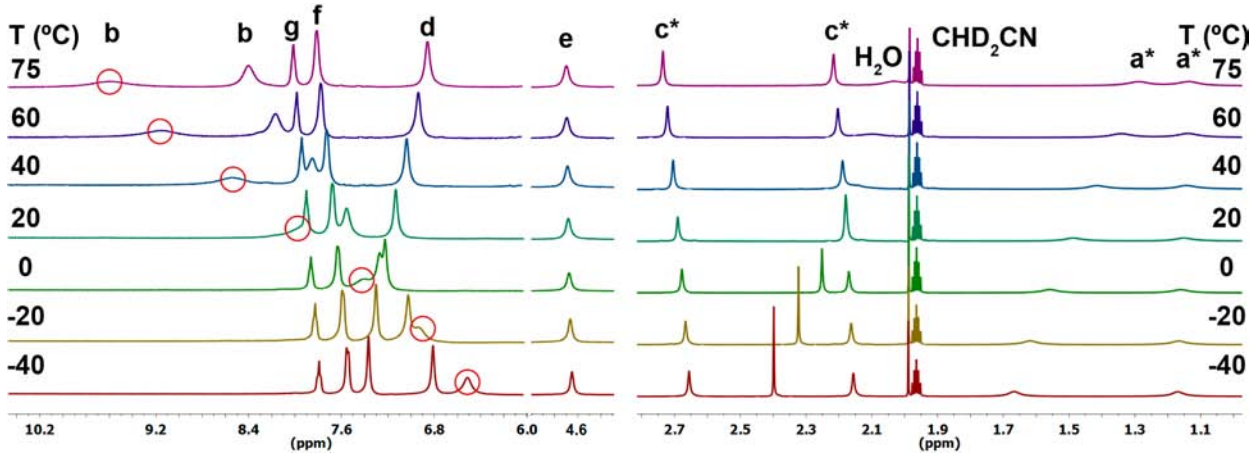

Figure 3. Variable-temperature (VT) ^{1}H NMR spectra of $[Cu_2(\mu\text{-Br})(\mu\text{-L}_m\text{*})_2](ClO_4)_3$. The red circles mark the position of one of the two nonequivalent *b*-pyrazolyl resonances at each temperature. This resonance was used for the calculation of $-J$ in solution. The resonance for the small amount of H_2O (δ = 2.40 ppm at −40 °C) present in CD_3CN broadens with increasing temperature and overlaps with one *c** resonance at 20 °C.

Table 2. Spin−Lattice (Longitudinal) Relaxation Times (T_1), Cu···H Distances Calculated from T_1 in Solution and Cu···H Distances from the Single-Crystal X-ray Diffraction Structures[9a] for $[Cu_2(\mu\text{-Br})(\mu\text{-L}_m\text{*})_2](ClO_4)_3$

		$d_{Cu\cdots H}$ (Å)		
δ (ppm) at 20 °C	T_1 (ms) at −40 °C	NMR	cryst	assignment[a]
1.49	16.87	3.80	3.78	*a** (eq)
1.15	15.04	3.73	3.69	*a** (ax)
2.18	116.90	5.26	5.84	*c** (ax)
2.69	138.00	5.40	5.91	*c** (eq)
4.69	20.91	3.94	4.07	*e*
7.13	30.46	4.20	4.25	*d*
7.56	70.66	4.83	5.06	*b* (ax)
7.68	38.67	used as ref	4.37	*f*
7.91	92.73	5.06	5.76	*g*
8.00	75.52	4.89	5.17	*b* (eq)

[a]Axial and equatorial assignments are tentative.

be found in the Supporting Information (Tables S1−S4), demonstrating that the *correlation* of solid-state and solution structures is *general* for this class of complexes.

The ^{1}H−^{13}C HSQC spectra of $[Cu_2(\mu\text{-Br})(\mu\text{-L}_m\text{*})_2](ClO_4)_3$, recorded at 20 °C, clearly correlate the proton and carbon resonances (Figure 4). No correlations were found for the *b*-pyrazolyl resonances, probably a result of short nuclear relaxation times. These *b*-pyrazolyl resonances are also absent in the ^{13}C NMR spectra.

Similar assignments were made for $[Cu_2(\mu\text{-OH})(\mu\text{-L}_m\text{*})_2](ClO_4)_3$, the VT NMR spectra is shown in Figure S1 in the Supporting Information. The ^{1}H−^{13}C HSQC spectra at 20 °C confirms that the *g* and *f* resonances are merged in the ^{1}H NMR spectrum (8.52 ppm). The most prominent difference in the ^{1}H−^{13}C HSQC spectra of the bromide and the hydroxide bridged compounds is a cross peak at δ(7.57,124.1) that can be assigned to one of the *b*-pyrazolyl resonances (allowing the assignment of one ^{13}C *b* resonance in Table 1), while the proton−carbon cross peak for resonance *e* disappears (Figure 5). The proof that δ(7.57,124.1) corresponds to a *b*-pyrazolyl resonance, and not the *e*, comes from the ^{1}H−^{13}C HSQC experiment at −40 °C, where this cross peak shifts to δ(6.72,115.4), and the ^{1}H−^{13}C HMBC experiment which correlates the ^{13}C resonance at 115.4 ppm with one *c**-pyrazolyl resonance at 2.67 ppm (Figure 6, blue circle). The Cu···H distances calculated from T_1 also confirm that the resonance at 7.57 ppm corresponds to *b* ($d_{Cu\cdots H}$ NMR vs. cryst: 5.14 Å vs. 5.25 Å), while the resonance at 3.95 ppm corresponds to *e* ($d_{Cu\cdots H}$ NMR vs. cryst: 3.63 Å vs. 4.07 Å) (see Table S1 in the Supporting Information).

In the ^{13}C NMR spectra of the $[Cu_2(\mu\text{-X})(\mu\text{-L}_m\text{*})_2](ClO_4)_3$ series, we were unable to observe the quaternary *a*, *c*, and some of the *b*-pyrazolyl carbon resonances at 20 °C, but the ^{1}H−^{13}C HMBC spectrum of $[Cu_2(\mu\text{-OH})(\mu\text{-L}_m\text{*})_2](ClO_4)_3$ at −40 °C indicates that these resonances have chemical shifts in a similar range as $[Cd_2(\mu\text{-F})(\mu\text{-L}_m\text{*})_2](BF_4)_3$,[9c] 145−154 ppm (see green circles in Figure 6). These resonances would be more

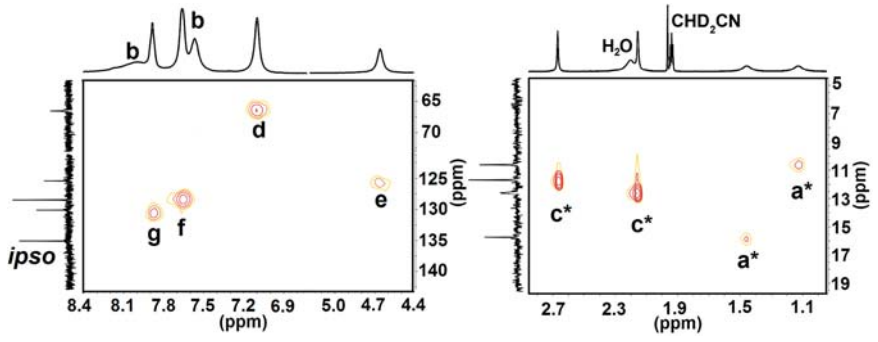

Figure 4. ^{1}H−^{13}C HSQC spectra of $[Cu_2(\mu\text{-Br})(\mu\text{-L}_m\text{*})_2](ClO_4)_3$ at 20 °C.

dx.doi.org/10.1021/ic402016m | *Inorg. Chem.* 2013, 52, 12741−12748

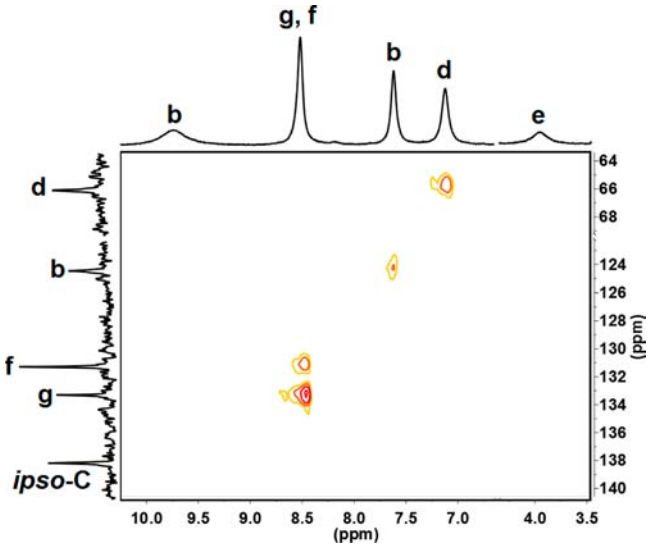

Figure 5. Fragment of the $^{1}H-^{13}C$ HSQC spectrum of $[Cu_2(\mu\text{-}OH)(\mu\text{-}\mathbf{L}_m{}^*)_2](ClO_4)_3$ at 20 °C.

shifted for the more weakly antiferromagnetically coupled compounds.

For $[Cu_2(\mu\text{-}Cl)(\mu\text{-}\mathbf{L}_m{}^*)_2](ClO_4)_3$, the $^{1}H-^{13}C$ HSQC spectrum shows a cross peak for the merged *g* and *f* resonances δ(8.19,130.3), δ(8.19,131.9) and two cross peaks for the *c** resonances δ(2.70,14.8), δ(1.93,18.3). The other resonances can be assigned based on similar assignments for $[Cu_2(\mu\text{-}Br)(\mu\text{-}\mathbf{L}_m{}^*)_2](ClO_4)_3$, the VT NMR spectra (see Figure S2 in the Supporting Information) and T_1 measurements.

The compound $[Cu_2(\mu\text{-}F)(\mu\text{-}\mathbf{L}_m{}^*)_2](ClO_4)_3$ behaves similarly to $[Cu_2(\mu\text{-}Cl)(\mu\text{-}\mathbf{L}_m{}^*)_2](ClO_4)_3$ (Figure S3 in the Supporting Information). For $[Cu_2(\mu\text{-}CN)(\mu\text{-}\mathbf{L}_m{}^*)_2](ClO_4)_3$, the NMR data and T_1 measurements are inconclusive, regarding the assignment of the resonances (Figure S4 in the Supporting Information).

The VT ^{1}H NMR spectra of $[Cu_2(\mu\text{-}X)(\mu\text{-}\mathbf{L}_m)_2](A)_3$ (X = F^-, A = BF_4^-; X = Cl^-, OH^-, A = ClO_4^-) are shown in Figure 7, as well as in Figures S5 and S6 in the Supporting Information. These compounds behave similarly to their

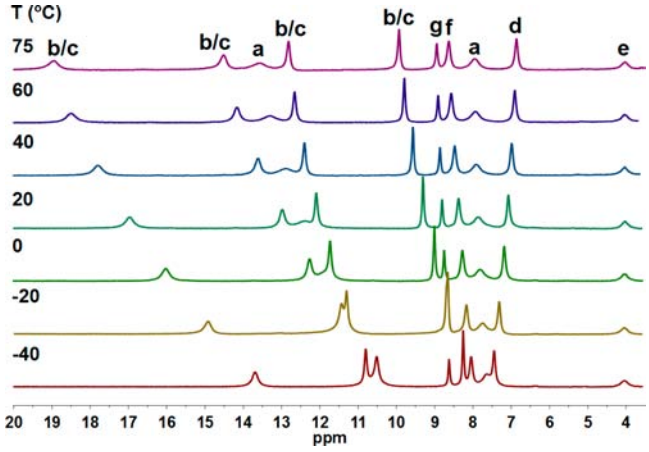

Figure 7. VT ^{1}H NMR spectra of $[Cu_2(\mu\text{-}OH)(\mu\text{-}\mathbf{L}_m)_2](ClO_4)_3$.

analogues with the $\mathbf{L}_m{}^*$ ligand, except the unsubstituted pyrazolyl ring resonances make the assignments more difficult because they are observed in the same region as the other resonances; the T_1 measurements become crucial (see Tables S5–S7 in the Supporting Information). The pyrazolyl rings show two very broad pyrazolyl resonances in the ^{13}C NMR spectra of the OH^- and F^- bridged compounds (see Table 1). The $^{1}H-^{13}C$ HSQC experiment shows five correlations for $[Cu_2(\mu\text{-}OH)(\mu\text{-}\mathbf{L}_m)_2](ClO_4)_3$ corresponding to the *d*, *f*, *g*, and two pyrazolyl hydrogen atoms, despite the weaker antiferromagnetic interactions (see Figure S7 in the Supporting Information), for $[Cu_2(\mu\text{-}Cl)(\mu\text{-}\mathbf{L}_m)_2](ClO_4)_3$ three correlations, *d*, *f*, and *g*, while for $[Cu_2(\mu\text{-}F)(\mu\text{-}\mathbf{L}_m)_2](ClO_4)_3$ four correlations, *d*, *f*, *g*, and a pyrazolyl hydrogen. The $^{1}H-^{1}H$ COSY experiments failed for these compounds. In three different sample of $[Cu_2(\mu\text{-}F)(\mu\text{-}\mathbf{L}_m)_2](ClO_4)_3$, the resonances of $[Cu_2(\mu\text{-}OH)(\mu\text{-}\mathbf{L}_m)_2](ClO_4)_3$ were identified (see Figure S6 in the Supporting Information). These resonances grow over time, suggesting that the water in the solvent is promoting the exchange of the F^- and OH^- bridges in solution.

Determination of the Exchange Coupling Constant (−*J*) from VT NMR. The population of the paramagnetic triplet (S = 1) and diamagnetic singlet (S = 0) states is

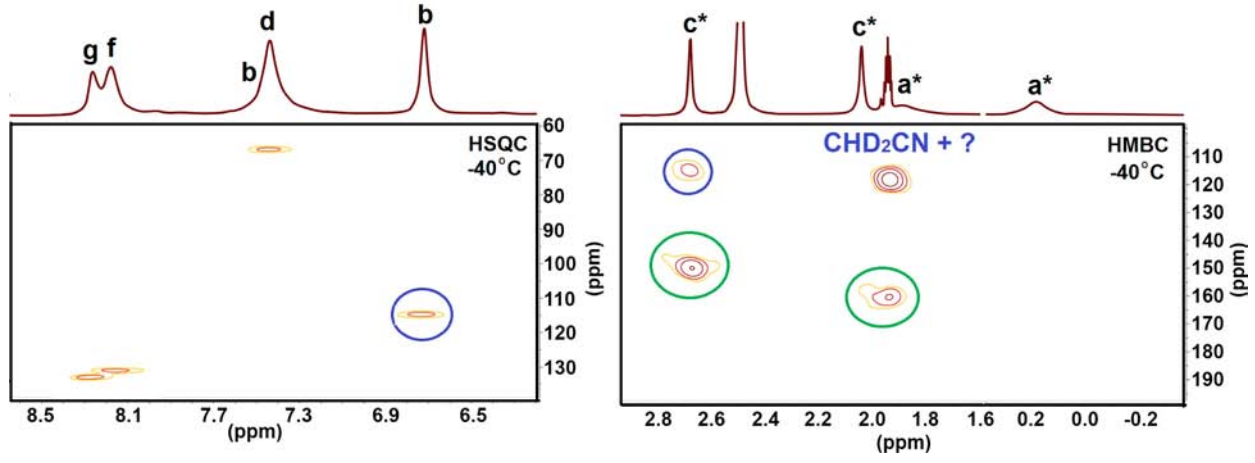

Figure 6. Fragments of the $^{1}H-^{13}C$ HSQC and $^{1}H-^{13}C$ HMBC spectra of $[Cu_2(\mu\text{-}OH)(\mu\text{-}\mathbf{L}_m{}^*)_2](ClO_4)_3$ at −40 °C. The cross peak δ(6.72,115.4) in the $^{1}H-^{13}C$ HSQC and δ(2.67,114.5) in the $^{1}H-^{13}C$ HMBC spectra are marked by a blue circle (a second cross peak at ∼115 ppm might be overlapped by the solvent (CHD_2CN) cross peak). The green circles show the two bond correlation of the *a**, *c**-pyrazolyl proton resonances with *a*- and *c*-pyrazolyl ^{13}C resonances (these ^{13}C resonances could not be observed at 20 °C).

dx.doi.org/10.1021/ic402016m | *Inorg. Chem.* 2013, 52, 12741−12748

temperature-dependent, which is a change that impacts the ^{1}H NMR spectra. The energy difference between these states corresponds to $-J$, where $\hat{\mathbf{H}} = -J\hat{\mathbf{S}}_1\hat{\mathbf{S}}_2$. The temperature-dependent hyperfine shifts correlate with $-J$, according to the following equation:[7e,g,12]

$$\delta_{iso} = A\frac{g\beta}{g_N\beta_N k}\frac{e^{J/kT}}{T(1 + 3e^{J/kT})} + \delta_0$$

where δ_{iso} is the chemical shift of any ^{1}H NMR resonance, g the g-factor determined for the compounds in solid state (~2.15), β the Bohr magneton, g_N the nuclear g-factor, β_N the nuclear magneton, A the hyperfine coupling constant, k the Boltzmann constant, T the temperature, and δ_0 the hypothetical very low temperature position of the resonance chosen for the analyses. The chemical shifts of the resonances that show the largest temperature dependence (in all but one case, the *b*-pyrazolyl resonance; see Figure 3) were used for the analysis. After estimating δ_0 by letting it vary freely for $[Cu_2(\mu\text{-Br})(\mu\text{-}\mathbf{L}_m\text{*})_2](ClO_4)_3$, we fixed δ_0 at 5.6 ppm for the $\mathbf{L}_m$* and 6.1 ppm for $\mathbf{L}_m$ compounds, close to the chemical shift of the *b*-pyrazolyl resonance in the ligands $\mathbf{L}_m$* (5.8 ppm)[9c] and $\mathbf{L}_m$ (6.3 ppm)[9d] at room temperature.[13] The parameters $-J$ and A were simultaneously fit (Table 3) to the equation above with the software SigmaPlot. Observed and calculated chemical shifts are shown in Table S8 in the Supporting Information. We repeated the fitting procedure for each compound with other resonances and obtained similar $-J$ values in each case (see Figure S8 and Table S9 in the Supporting Information). The A values match the literature values for other copper(II) compounds.[14]

Table 3. Results of the Fitting Procedure for $[Cu_2(\mu\text{-X})(\mu\text{-}\mathbf{L}_m)_2](A)_3$ (X = F^-, A = BF_4^-; X = Cl^-, OH^-, A = ClO_4^-) and $[Cu_2(\mu\text{-X})(\mu\text{-}\mathbf{L}_m\text{*})_2](ClO_4)_3$ (X = CN^-, F^-, Cl^-, OH^-, Br^-)

compound	δ_{iso} (ppm) at 20 °C[a]	A (MHz) solution[b]	$-J$ (cm^{-1}) solution[b]	$-J$ (cm^{-1}) solid state
$[Cu_2(\mu\text{-F})(\mu\text{-}\mathbf{L}_m)_2](BF_4)_3$	29.71	1.68 (±0.2)	338 (±2)	365[d]
$[Cu_2(\mu\text{-Cl})(\mu\text{-}\mathbf{L}_m)_2](ClO_4)_3$	24.55	1.99 (±0.3)	460 (±3)	536
$[Cu_2(\mu\text{-OH})(\mu\text{-}\mathbf{L}_m)_2](ClO_4)_3$	14.92	1.63 (±0.2)	542 (±3)	555
$[Cu_2(\mu\text{-CN})(\mu\text{-}\mathbf{L}_m\text{*})_2](ClO_4)_3$	17.66[c]	0.45 (±0.3)	128 (±12)	160
$[Cu_2(\mu\text{-F})(\mu\text{-}\mathbf{L}_m\text{*})_2](ClO_4)_3$	26.85	1.47 (±0.3)	329 (±2)	340
$[Cu_2(\mu\text{-Cl})(\mu\text{-}\mathbf{L}_m\text{*})_2](ClO_4)_3$	12.10	2.04 (±0.3)	717 (±4)	720
$[Cu_2(\mu\text{-OH})(\mu\text{-}\mathbf{L}_m\text{*})_2](ClO_4)_3$	9.77	1.98 (±0.6)	823 (±7)	808
$[Cu_2(\mu\text{-Br})(\mu\text{-}\mathbf{L}_m\text{*})_2](ClO_4)_3$	8.00	2.15 (±0.4)	944 (±4)	945

[a]Resonances assigned to the *b*-pyrazolyl hydrogens except for $[Cu_2(\mu\text{-CN})(\mu\text{-}\mathbf{L}_m\text{*})_2](ClO_4)_3$, where the assignment is not possible, but is not the *b*-pyrazolyl resonance, based on the A value. [b]R_{fit}^2 = 0.97–0.99. [c]δ_0 = 7.07 ppm. [d]In ref 9b, the $-2J$ convention was used to define the singlet–triplet energy gap.

Although the freezing and boiling point of the solvent restrict the data collection to a relatively narrow temperature range, the error margins are relatively small (see Figure 8 and Table 3). The results of the fit are in good agreement with the $-J$ values determined in the solid state, the difference between the solid-state and solution $-J$ values being between 1 to 32 cm^{-1}, except for $[Cu_2(\mu\text{-Cl})(\mu\text{-}\mathbf{L}_m)_2](ClO_4)_3$. This good agreement between the $-J$ values indicates that the linear or near-linear Cu–X–Cu angle in the solid state is retained in solution for most compounds, and the geometry around the copper(II) centers remains largely unchanged. The successful determination of $-J$ in solution for this extensive series of complexes in which the bridging group is varied demonstrates the *power of the method* and provides an *alternative route* for the correlation of solid and solution structures.

The data for $[Cu_2(\mu\text{-OH})(\mu\text{-}\mathbf{L}_m)_2](ClO_4)_3$ is especially interesting in the light of the bent Cu–O–Cu angle in the solid state (142°), resulting in a geometry around copper(II) that is better described as distorted axially elongated square pyramidal than trigonal bipyramidal. The excellent agreement between $-J$ in solution (542 cm^{-1}) and in the solid state (555 cm^{-1}) for $[Cu_2(\mu\text{-OH})(\mu\text{-}\mathbf{L}_m)_2](ClO_4)_3\cdot 2H_2O$ suggests that the bridging angle and distorted square pyramidal geometry is retained in solution.

The solution $-J$ value for $[Cu_2(\mu\text{-Cl})(\mu\text{-}\mathbf{L}_m)_2](ClO_4)_3$ differs by 76 cm^{-1} from the solid-state value, a difference that is larger than that for the other compounds, and what can be explained by experimental error. A possible explanation is that, in this case, the solution structure is different from that in the solid state. In the crystal structure, there are two independent molecules in 1:1 ratio:[10] one with a bent Cu–Cl–Cu angle of 138.5°, and another that is more linearly bridged (167.8°). It is likely that, in the solution state, there is a difference in the bridging angle, compared to the average angle in the solid state, resulting in lower $-J$ values in solution.

Density functional theory (DFT) calculations were performed on $[Cu_2(\mu\text{-Br})(\mu\text{-}\mathbf{L}_m\text{*})_2](ClO_4)_3$ with the software ORCA[15] to estimate the magnitude of A for the *b*-pyrazolyl hydrogens. The calculated A values for all other compounds should be similar to that of $[Cu_2(\mu\text{-Br})(\mu\text{-}\mathbf{L}_m\text{*})_2](ClO_4)_3$, because the spin densities on the corresponding hydrogens are similar.[9a] Ahlrichs-type basis set TZVPP for copper(II) and SVP for other atoms were used, combined with the B3LYP functional.[16] Ahlrichs polarization functions from basis H–Kr R and auxiliary bases from the TurboMole library were also used.[17] The bromide bridged molecule was simplified by removal of the methyl groups on the pyrazolyl fragments, as well as the benzene rings, and hydrogen atoms were placed at appropriate positions. All remaining atoms were retained at the positions determined by X-ray crystallography. The calculations result in an average A value of 0.65 MHz for the equatorial and 1.43 MHz for the axial *b*-pyrazolyl hydrogens,[18] which is consistent with the literature data.[14] The fitting of the experimental data (see Table S8 in the Supporting Information), results in a similar A value, 2.15 (±0.4) MHz, for the axial *b*-pyrazolyl hydrogens (see Table 3).

We also note that the *d* methine hydrogens should have negative A values, because the resonance of the *d* hydrogen is moving to higher shielding with increasing temperature in the VT ^{1}H NMR spectra (see Figure 3). We have fitted the $[Cu_2(\mu\text{-Br})(\mu\text{-}\mathbf{L}_m\text{*})_2](ClO_4)_3$ data using the *d* hydrogens and the result, A = −0.34 MHz (see Figure S8 and Table S9 in the Supporting Information), is similar to that calculated by ORCA (A = −0.30 MHz).

CONCLUSIONS

The ^{1}H and ^{13}C NMR, in combination with two-dimensional (2D) NMR correlation spectroscopy and T_1 relaxation time measurements, have been used to study the structure and

dx.doi.org/10.1021/ic402016m | Inorg. Chem. 2013, 52, 12741–12748

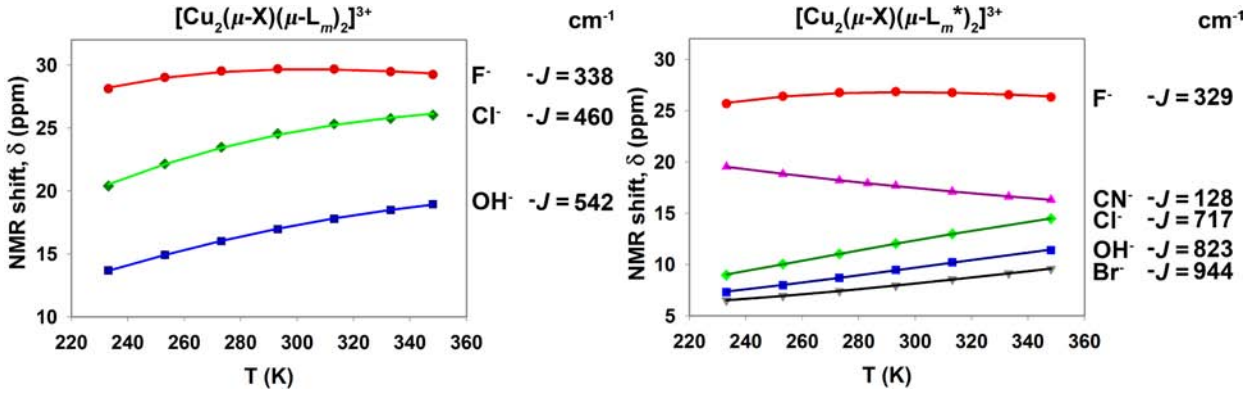

Figure 8. Plot of chemical shifts (δ) of the *b*-pyrazolyl resonances versus the temperature (233−348 K). In the case of $[Cu_2(\mu\text{-CN})(\mu\text{-}\mathbf{L}_m^*)_2](ClO_4)_3$, the plotted resonance could not be identified. Fitting of the experimental data (represented by the symbols) results in the solid lines (R_{fit}^2 = 0.97−0.99). The $-J$ values are shown on the right side of the plots.

properties of antiferromagnetically coupled, dinuclear copper(II) compounds in solution, despite the large variation in the strength of the antiferromagnetic interactions. Even though the nuclear relaxation times are short, the $^1H-^1H$ COSY and especially the $^1H-^{13}C$ HMBC experiments result in limited, but clearly useful, information for compounds with $-J > 700$ cm^{-1}, particularly at lower temperatures. We were able to observe correlations in the $^1H-^{13}C$ HSQC spectra for compounds with $-J > 500$ cm^{-1}. The T_1 measurements accurately determine the Cu···H distances in these molecules. The analyses of the data lead to the conclusion that the dinuclear structure and the unusual axially compressed trigonal bipyramidal geometry are retained in CD_3CN for the $\mathbf{L}_m^*$ series, complexes that have the linear Cu−X−Cu arrangement. The structure in solution of the complexes in the $\mathbf{L}_m$ series, which have bent Cu−X−Cu bridges, are also similar to the solid state, although, for $[Cu_2(\mu\text{-Cl})(\mu\text{-}\mathbf{L}_m)_2](ClO_4)_3$, there may be some variation.

This study is the first where the VT NMR method was used for determination of $-J$ in solution for an extended series of antiferomagnetically coupled, dinuclear paramagnetic copper(II) compounds, where the bridging anion (X) was systematically varied. The solution and solid-state $-J$ values are very similar, showing that these compounds retain their solid-state structures in solution. The VT NMR method was shown to be extremely useful for the determination of solution state $-J$ values over a large range of antiferromagnetic interactions with different strengths, from 944 cm^{-1} to 128 cm^{-1}.

■ ASSOCIATED CONTENT

Supporting Information

VT ^1H NMR spectra, T_1 measurments, $^1H-^{13}C$ HSQC spectrum of $[Cu_2(\mu\text{-OH})(\mu\text{-}\mathbf{L}_m)_2](ClO_4)_3$, experimental and calculated chemical shifts for the fitted data, results of the fit for $[Cu_2(\mu\text{-Br})(\mu\text{-}\mathbf{L}_m^*)_2](ClO_4)_3$ using the *d* methine resonance. This material is available free of charge via the Internet at http://pubs.acs.org.

■ AUTHOR INFORMATION

Corresponding Author

*Tel.: 803-777-2587. Fax: 803-777-9521. E-mail reger@mailbox.sc.edu.

Notes

The authors declare no competing financial interest.

■ ACKNOWLEDGMENTS

The authors acknowledge with thanks the financial support of the National Science Foundation (through Grant No. CHE-1011736). The NHMFL is funded by the NSF through the Cooperative Agreement No. DMR-1157490, the State of Florida, and the DOE.

■ REFERENCES

(1) (a) Rolff, M.; Schottenheim, J.; Decker, H.; Tuczek, F. *Chem. Soc. Rev.* **2011**, *40*, 4077−4098. (b) Koval, I. A.; Gamez, P.; Belle, C.; Selmeczi, K.; Reedijk, J. *Chem. Soc. Rev.* **2006**, *35*, 814−840. (c) Rolff, M.; Schottenheim, J.; Tuczek, F. *J. Coord. Chem.* **2010**, *63*, 2382−2399. (d) Coughlin, P. K.; Lippard, S. J. *J. Am. Chem. Soc.* **1981**, *103*, 3228−3229. (e) Selmeczi, K.; Règlier, M.; Giorgi, M.; Speier, G. *Coord. Chem. Rev.* **2003**, *245*, 191−201.

(2) (a) Yoon, J.; Fujii, S.; Solomon, E. I. *Proc. Natl. Acad. Sci.* **2009**, *106*, 6585−6590. (b) Claus, H.; Decker, H. *Syst. Appl. Microbiol.* **2006**, *29*, 3−14. (c) Li, Y.; Wang, Y.; Jiang, H.; Deng, J. *Proc. Natl. Acad. Sci.* **2009**, *106*, 17002−17006. (d) Gerdemann, C.; Eicken, C.; Krebs, B. *Acc. Chem. Res.* **2002**, *35*, 183−191. (e) Eicken, C.; Krebs, B.; Sacchetini, J. C. *Curr. Opin. Struct. Biol.* **1999**, *9*, 677−683. (f) Peisach, J.; Aisen, P.; Blumberg, W. E. *The Biochemistry of Copper*; Academic Press: New York, 1966. (g) Zaballa, M.-E.; Ziegler, L.; Kosman, D. J.; Vila, A. J. *J. Am. Chem. Soc.* **2010**, *132*, 11191−11196. (h) Abriata, L. A.; Ledesma, G. N.; Pierattelli, R.; Vila, A. J. *J. Am. Chem. Soc.* **2009**, *131*, 1939−1946. (i) Fernández, C. O.; Vila, A. J. Paramagnetic NMR of Electron Transfer Copper Proteins. In *Paramagnetic Resonance of Metallobiomolecules*; ACS Symposium Series *858*; American Chemical Society: Washington, DC, 2003; pp 287−303. (j) Donaire, A.; Jiménez, B.; Fernández, C. O.; Pierattelli, R.; Niizeki, T.; Moratal, J.-M.; Hall, J. F.; Kohzuma, T.; Hasnain, S. S.; Vila, A. J. *J. Am. Chem. Soc.* **2002**, *124*, 13698−13708.

(3) (a) Kahn, O. *Molecular Magnetism*; VCH Publishers, Inc.: New York, 1993. (b) Hay, P. J.; Thibeault, J. C.; Hoffmann, R. *J. Am. Chem. Soc.* **1975**, *97*, 4884−4899.

(4) (a) Pinkowicz, D.; Chorąży, S.; Olaf, S. *Sci. Progress* **2011**, *94*, 139−183. (b) Miller, J. S.; Gatteschi, D. *Chem. Soc. Rev.* **2011**, *40*, 3065−3066. (c) Leuenberger, M. N.; Loss, D. *Nature* **2001**, *410*, 789−793. (d) Kahn, O. *Acc. Chem. Res.* **2000**, *33*, 647−657. (e) Wernsdorfer, W.; Aliaga−Alcalde, N.; Hendrickson, D. N.; Christou, G. *Nature* **2002**, *416*, 406−409.

(5) (a) Nùñez, C.; Bastida, R.; Macías, A.; Valencia, L.; Neuman, N. I.; Rizzi, A. C.; Brondino, C. D.; González, P. J.; Capelo, J. L.; Lodeiro, C. *Dalton Trans.* **2010**, *39*, 11654−11663. (b) Mutti, F. G.; Zoppellaro, G.; Gulotti, M.; Santagostini, L.; Pagliarin, R.; Andersson, K. K.; Casella, L. *Eur. J. Inorg. Chem.* **2009**, 554−556 and references therein. (c) Solomon, E. I.; Ginsbach, J. W.; Heppner, D. E.; Kieber−Emmons, M. T.; Kjaergaard, C. H.; Smeets, P. J.; Tian,

L.; Woertink, J. S. *Faraday Discuss.* **2010**, *148*, 11−39. (d) Battaini, G.; Granata, A.; Monzani, E.; Gullotti, M.; Casella, L. *Adv. Inorg. Chem.* **2006**, *58*, 185−233. (e) Siegbahn, P. E. M. *Faraday Discuss.* **2003**, *124*, 289−296. (f) Pirngruber, G. D.; Frunz, L.; Lüchinger, M. *Phys. Chem. Chem. Phys.* **2009**, *11*, 2928−2938. (g) Bertini, I.; Gray, H. B.; Lippard, S. J.; Valentine, J. S. *Bioinorganic Chemistry*; University Science Books: Mill Valley, CA, 1994. (h) Liu, H. Y.; Scharbert, B.; Holm, R. H. *J. Am. Chem. Soc.* **1991**, *113*, 9529−9539.

(6) (a) Bertini, I.; Turano, P.; Vila, A. J. *Chem. Rev.* **1993**, *93*, 2833−2932. (b) Machonkin, T. E.; Westler, W. M.; Markley, J. L. *Inorg. Chem.* **2005**, *44*, 779−797. (c) Holm, R. H.; Abbott, E. H. In *Coordination Chemistry*; Martell, A. E., Ed.; Van Nostrand Reinhold Company: New York, 1971; Vol. *2*, pp 264−340. (d) Clementi, V.; Luchinat, C. *Acc. Chem. Res.* **1998**, *31*, 351−361.

(7) (a) Tanase, S.; Koval, I . A.; Bouwman, E.; de Gelder, R.; Reedijk, J. *Inorg. Chem.* **2005**, *44*, 7860−7865. (b) Satcher, J. H.; Balch, A. L. *Inorg. Chem.* **1995**, *34*, 3371−3373. (c) Holz, R. C.; Bradshow, J. M.; Bennett, B. *Inorg. Chem.* **1998**, *37*, 1219−1225. (d) Holz, R. C.; Brink, J. M.; Gobena, F. T.; O'Connor, C. J. *Inorg. Chem.* **1994**, *33*, 6086−6092. (e) Maekawa, M.; Kitagawa, S.; Munakata, M.; Masuda, H. *Inorg. Chem.* **1989**, *28*, 1904−1909. (f) Mandal, P. K.; Manoharan, P. T. *Inorg. Chem.* **1995**, *34*, 270−277. (g) Asokan, A.; Varghese, B.; Manoharan, P. T. *Inorg. Chem.* **1999**, *38*, 4393−4399. (h) Gupta, R.; Mukherjee, S.; Mukherjee, R. *J. Chem. Soc., Dalton Trans.* **1999**, 4025−4030.

(8) (a) Koval, I. A.; van der Schilden, K.; Schuitema, A. M.; Gamez, P.; Belle, C.; Pierre, J.-L.; Lüken, M.; Krebs, B.; Roubeau, O.; Reedijk, J. *Inorg. Chem.* **2005**, *44*, 4372−4382. (b) Mohanta, S.; Adhikary, B.; Baitalik, S.; Nag, K. *New J. Chem.* **2001**, *25*, 1466−1471. (c) Murthy, N. N.; Karlin, K. D.; Bertini, I.; Luchinat, C. *J. Am. Chem. Soc.* **1997**, *119*, 2156−2162. (d) Lubben, M.; Hage, R.; Meetsma, A.; Bÿma, K.; Feringa, B. L. *Inorg. Chem.* **1995**, *34*, 2217−2224. (e) Brink, J. M.; Rose, R. A.; Holz, R. C. *Inorg. Chem.* **1996**, *35*, 2878−2885. (f) Holz, R. C.; Brink, J. M. *Inorg. Chem.* **1994**, *33*, 4609−4610.

(9) (a) Reger, D. L.; Pascui, A. E.; Smith, M. D.; Jezierska, J.; Ozarowski, A. *Inorg. Chem.* **2012**, *51*, 7966−7968. (b) Reger, D. L.; Foley, E. A.; Watson, R. P.; Pellechia, P. J.; Smith, M. D.; Grandjean, F.; Long, G. J. *Inorg. Chem.* **2009**, *48*, 10658−10669. (c) Reger, D. L.; Pascui, A. E.; Smith, M. D.; Jezierska, J.; Ozarowski, A. *Inorg. Chem.* **2012**, *51*, 11820−11836. (d) Reger, D. L.; Watson, R. P.; Smith, M. D.; Pellechia, P. J. *Organometallics* **2005**, *24*, 1544−1555. (e) Reger, D. L.; Pascui, A. E.; Pellechia, P. J.; Smith, M. D. *Inorg. Chem.* **2013**, *52*, 11638−11649.

(10) The crystallographic unit cell of these acetonitrile solvated compounds contain two independent $[Cu_2(\mu\text{-Cl})(\mu\text{-}\mathbf{L}_m)_2]^{3+}$ cations.

(11) (a) *MestReNOVA 5.2.5*, Mestrelab Research S.L., 2008. (b) *SigmaPlot 11.0*, Systat Software, Inc., 2008.

(12) Pfirrmann, S.; Limberg, C.; Herwig, C.; Knispel, C.; Braun, B.; Bill, E.; Stösser, R. *J. Am. Chem. Soc.* **2010**, *132*, 13684−13691.

(13) For the compounds with large $-J$, e.g. $[Cu_2(\mu\text{-Br})(\mu\text{-}\mathbf{L}_m{}^*)_2](ClO_4)_3$, the temperature dependence of the chemical shifts is very small and δ_0 becomes critical.

(14) Sharples, K. M.; Carter, E.; Hughes, C. E.; Harris, K. D. M.; Platts, J. A.; Murphy, D. M. *Phys. Chem. Chem. Phys.* **2013**, *15*, 15214−15222.

(15) (a) Neese, F. *ORCA—An ab initio, Density Functional and Semiempirical Program Package*, Version 2.9.1, 2012. (b) Neese, F. *Comput. Mol. Sci.* **2012**, *2*, 73−78.

(16) (a) Becke, D. A. *Phys. Rev. A* **1988**, *38*, 3098−3100. (b) Perdew, J. P. *Phys. Rev. B* **1986**, *33*, 8822−8824. (c) Perdew, J. P. *Phys. Rev. B.* **1986**, *34*, 7406−7406. (d) Kendall, R. A.; Früchtl, H. A. *Theor. Chem. Acc.* **1997**, *97*, 158−163.

(17) (a) Schaefer, A.; Horn, H.; Ahlrichs, R. *J. Chem. Phys.* **1992**, *97*, 2571−2577. (b) Ahlrichs, R. et al., unpublished results. The Ahlrichs auxiliary basis sets were obtained from the TurboMole basis set library under ftp.chemie.uni-karlsruhe.de/pub/jbasen.

(18) ORCA calculates two values for both axial and equatorial *b*-pyrazolyl hydrogens as the two sides of copper(II) coordination sphere are not equal in the X-ray structure. The molecule is more symmetric in solution than in solid state, we observe one axial (4H, red Figure 2) and equatorial (4H) *b*-pyrazolyl resonance.